RESEARCH REPORT

WNT/β-catenin signaling plays a crucial role in myoblast fusion through regulation of nephrin expression during development

Akiko Suzuki[1,2], Ryohei Minamide[1,2] and Junichi Iwata[1,2,3,*]

ABSTRACT

Skeletal muscle development is controlled by a series of multiple orchestrated regulatory pathways. WNT/β-catenin is one of the most important pathways for myogenesis; however, it remains unclear how this signaling pathway regulates myogenesis in a temporal- and spatial-specific manner. Here, we show that WNT/β-catenin signaling is crucial for myoblast fusion through regulation of the nephrin (*Nphs1*) gene in the *Myog-Cre*-expressing myoblast population. Mice deficient for the β-catenin gene in *Myog-Cre*-expressing myoblasts (*Ctnnb1$^{F/F}$;Myog-Cre* mice) displayed myoblast fusion defects, but not migration or cell proliferation defects. The promoter region of *Nphs1* contains the conserved β-catenin-binding element, and *Nphs1* expression was induced by the activation of WNT/β-catenin signaling. The induction of *Nphs1* in cultured myoblasts from *Ctnnb1$^{F/F}$;Myog-Cre* mice restored the myoblast fusion defect, indicating that nephrin is functionally relevant in WNT/β-catenin-dependent myoblast fusion. Taken together, our results indicate that WNT/β-catenin signaling is crucial for myoblast fusion through the regulation of the *Nphs1* gene.

KEY WORDS: WNT/β-catenin signaling, Muscle development, Myoblast fusion, Nephrin

INTRODUCTION

The multiple steps of muscle development and regeneration, beginning with muscle progenitor cell activation and ending with myofiber formation, are all subject to separate levels of regulation, and are affected in a variety of muscle disorders and atrophy conditions (Hutcheson et al., 2009). Clinically, individuals with muscle developmental defects have misoriented muscles and/or a delay in muscle development (Cohen et al., 1994). For example, a failure in the muscular development of the tongue, a muscular organ that plays important roles in feeding, swallowing, speech and respiration, results in increased risk for functional defects such as speech problems and swallowing difficulties (Carvajal Mornroy et al., 2012; Precious and Delaire, 1993). Individuals with a smaller tongue size [e.g. microglossia (also known as small tongue)] have more severe functional restrictions and there are currently no surgical treatment options. Therefore, individuals with muscle defects need long-term training in order to adjust to their conditions and may need additional surgical corrections after initial surgical

repair to acquire optimal functions (Dworkin et al., 2004; Perry, 2011). Despite the important physiological function of craniofacial muscles, the mechanism responsible for dysfunctional craniofacial muscle development is not well understood.

WNT signaling is essential for a variety of developmental and regenerative processes, including embryonic muscle development and maintenance of skeletal muscle homeostasis in the adult (Cisternas et al., 2014b; von Maltzahn et al., 2012a). In presence of WNT ligands, β-catenin is stabilized and translocates from the cytoplasm into the nucleus. Nuclear β-catenin forms a complex with transcriptional co-activators, such as members of the T-cell factor (TCF)/lymphoid enhancer-binding factor 1 (LEF1) family, to bind the promoter regions of target genes (Cisternas et al., 2014a). By contrast, in the absence of WNT ligands, a destruction complex, which consists of AXIN, adenomatous polyposis coli (APC) and the serine-threonine kinase glycogen synthase kinase 3 (GSK3β), is activated and phosphorylates β-catenin, leading to its degradation by the proteasome (MacDonald et al., 2009). During myogenesis, WNT/β-catenin signaling is activated in muscle cells, as shown in *BAT-gal* mice, in which seven TCF/LEF-binding sites drive nuclear *LacZ* expression in the presence of active β-catenin in the nuclei (Maretto et al., 2003), indicating that WNT/β-catenin signaling is activated in muscle cells. WNT ligands regulate the specification of skeletal myoblasts in the paraxial mesoderm, and induce location-specific expression of muscle regulatory factors (Cossu and Borello, 1999). WNT/β-catenin signaling is altered in multiple malformations and syndromes, including muscle disorders in humans (Al-Qattan, 2011; He and Chen, 2012; Kim and Vu, 2006). In individuals with muscular defects such as myopathies and atrophy, WNT/β-catenin signaling is most likely altered due to genetic and/or epigenetic factor(s) (Alexander et al., 2013). Mice with a conditional depletion of β-catenin in the muscle precursor *Pax7$^+$* cell lineage (*Ctnnb1$^{F/F}$;Pax7-Cre* mice) exhibit reduced muscle mass and slow myofibers (Hutcheson et al., 2009). Thus, dysregulation of WNT/β-catenin signaling in the mesoderm leads to both developmental defects and perturbation of muscle homeostasis. However, the spatiotemporal-specific roles of WNT/β-catenin signaling during myogenesis remain unclear.

In this study, we have identified muscle-specific WNT/β-catenin signaling molecules and downstream targets in mice deficient for β-catenin in the *Myog-Cre*-expressing myoblast population (*Ctnnb1$^{F/F}$; Myog-Cre* mice). Understanding the temporal-specific regulatory mechanism(s) for muscle biology (proliferation, differentiation and homeostasis) will not only advance our understanding of developmental biology, but could also provide new therapeutic and preventative approaches for muscle developmental defects as well as tissue engineering techniques for muscle regeneration.

RESULTS AND DISCUSSION
Developmental muscle defects in mice deficient for β-catenin
During fetal myogenesis, β-catenin positively regulates the number and type of progenitor cells and myofibers in mice with a conditional

[1]Department of Diagnostic and Biomedical Sciences, The University of Texas Health Science Center at Houston (UT Health) School of Dentistry, Houston, TX 77054, USA. [2]Center for Craniofacial Research, UT Health School of Dentistry, Houston, TX 77054, USA. [3]MD Anderson Cancer Center, UT Health Graduate School of Biomedical Sciences, Houston, TX 77054, USA.

*Author for correspondence (junichi.iwata@uth.tmc.edu)

A.S., 0000-0003-3163-8093; R.M., 0000-0001-8708-366X; J.I., 0000-0003-3975-6836

DEVELOPMENT

deletion of *Ctnnb1* in muscle progenitor cells (*Pax7$^{iCre/+}$;Ctnnb1$^{Δ/fl2-6}$* mice) (Hutcheson et al., 2009). In the subsequent stages of myoblast differentiation, WNT ligands are necessary and sufficient to induce the expression of *Myf5* and *MyoD* (*Myod1* – Mouse Genome Informatics) (Borello et al., 2006; Brunelli et al., 2007; Maroto et al., 1997; Munsterberg et al., 1995). Loss of β-catenin in the *Myf5*-expressing subpopulation leads to defects in myoblast migration and differentiation, whereas loss of β-catenin in the *MyoD*-expressing subpopulation causes no muscle developmental defect (Zhong et al., 2015). The molecular mechanism through which WNT/β-catenin signaling regulates late muscle developmental processes remains unclear. To investigate the final stage of muscle development, we analyzed mice with a β-catenin deficiency in differentiating muscles (*Ctnnb1$^{F/F}$;Myog-Cre* mice). We first confirmed that *Myog-Cre* is specifically expressed in all muscle cells by β-galactosidase staining in *Myog-Cre;R26R* mice (Fig. 1A). *Ctnnb1$^{F/F}$;Myog-Cre* mice died within 1 day of birth due to suckling and breathing defects (Fig. 1B;

Fig. S1C). Body weight was slightly decreased but not significantly changed in *Ctnnb1$^{F/F}$;Myog-Cre* mice compared with wild-type control littermates (Fig. 1C). We found that, among skeletal muscles, the tongues from *Ctnnb1$^{F/F}$;Myog-Cre* mice were smaller than the ones from control littermates (Fig. 1D,E). The reason why tongue size is most affected may be because the tongue muscles are the most matured skeletal muscles at birth, compared with the other muscles, because the tongue is used for suckling (Noden and Francis-West, 2006; Yamane, 2005). Interestingly, mice lacking both *Myf5* and *Pax3* exhibited skeletal muscle defects in the trunk and limbs, whereas the head muscles developed normally (Tajbakhsh et al., 1997). Although *Myf5*- and *MyoD*-null mice do not display any muscle defects, mice with a deficiency for both *Myf5* and *MyoD* lack almost all muscles at birth (Braun et al., 1992; Chen and Goldhamer, 2004; Kablar et al., 1997; Rudnicki et al., 1992, 1993). These findings suggest that muscle development may be regulated in a spatial-specific manner. In the tongue, mice with a deficiency
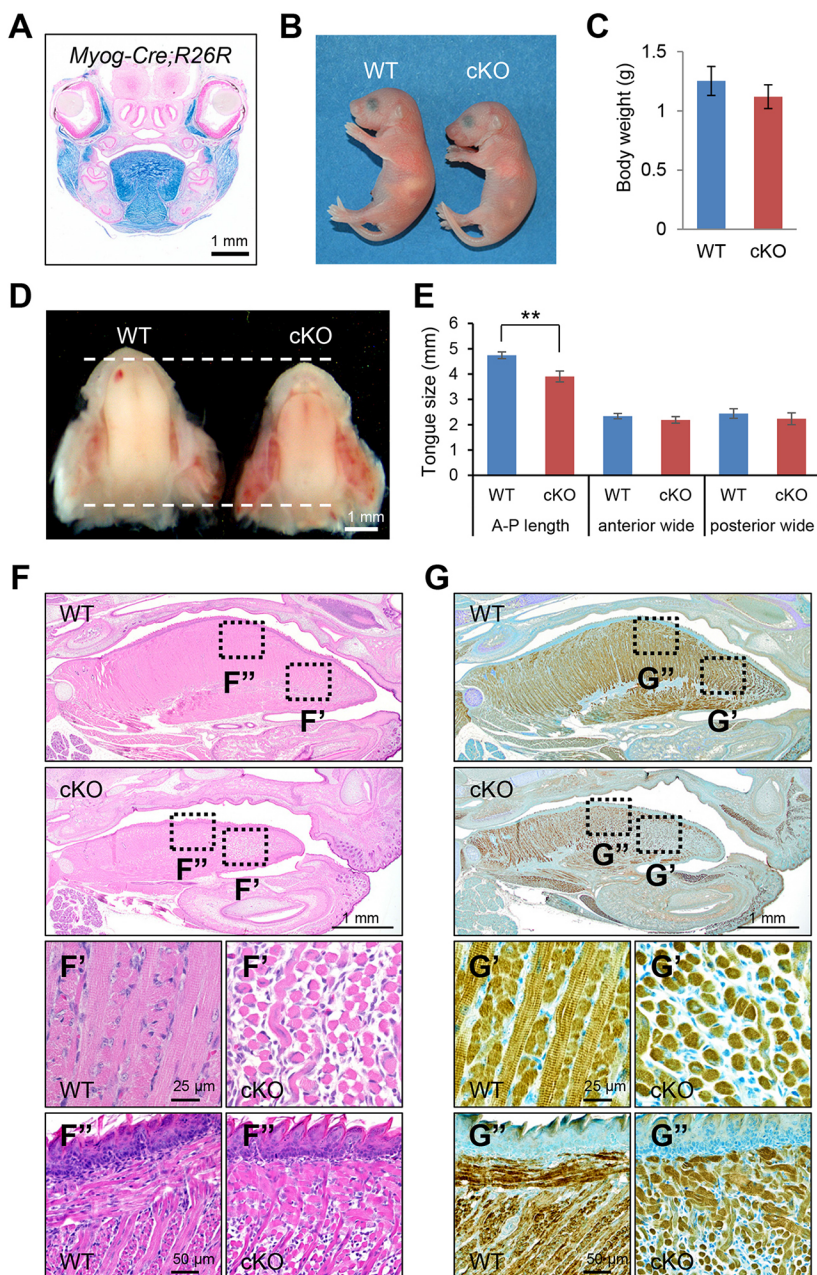

Fig. 1. WNT/β-catenin signaling is crucial for tongue muscle development. (A) β-Galactosidase staining of newborn *Myog-Cre:R26R* mice. Scale bar: 1 mm. (B) Gross picture of newborn wild-type (WT) control and *Ctnnb1* conditional null (cKO) mice. (C) Body weight of newborn WT control (blue bar) and cKO (red bar) mice. (D) Tongues from newborn WT and cKO mice. The dotted lines indicate either the anterior or posterior edge of the tongue. Scale bar: 1 mm. (E) Tongue size for WT control (blue bars) and cKO (red bars) mice in the anterior-posterior (A-P) axis length, anterior wide and posterior wide. **$P<0.01$. (F) Hematoxylin and Eosin staining of sagittal sections from newborn WT and cKO mice. The outlined areas (F′,F″) from WT and cKO images are enlarged in the lower panels. (G) Immunohistochemical staining for MYH in sagittal sections from newborn WT and cKO mice. The outlined areas (G′,G″) from WT and cKO images are enlarged in the lower panels. Scale bars: 1 mm in A,D,F,G; 50 μm in F″,G″; 25 μm in F′,G′.

for *Ctnnb1* in the *Myf5-Cre*-expressing myoblast population (*Ctnnb1^{F/F};Myf5-Cre* mice) display a myoblast migration defect, whereas mice with a deficiency for *Ctnnb1* in *Myod-Cre*-expressing myoblasts (*Ctnnb1^{F/F};Myod-Cre* mice), which constitute the majority of myoblasts in the tongue, exhibit no muscle developmental defect (Zhong et al., 2015). Mice with loss of myogenin (*Myog*), which is regulated by both *Myf5* and *Myod1*, have few myofibers because of a myoblast fusion defect (Hasty et al., 1993; Rawls et al., 1995), suggesting that almost all myoblasts express myogenin, which is crucial for the fusion process of muscle differentiation. To test whether muscle development is differentially affected by the location of muscles in *Ctnnb1^{F/F};Myog-Cre* mice, we performed histological analysis of the tongue, diaphragm and hindlimb muscles. We found that the size and number of muscle fibers were decreased in the tongue, diaphragm and hindlimb muscles from *Ctnnb1^{F/F};Myog-Cre* mice compared with controls (Fig. 1F,G). The diaphragm muscle is unique in mammals and is important for respiration. As expected, *Ctnnb1^{F/F};Myog-Cre* mice failed to fully expand the pulmonary alveoli at birth (Fig. S1). Our results suggest that WNT/β-catenin signaling is equally important in the *Myog-Cre*-expressing population during development.

Functional significance of WNT/β-catenin signaling in muscle cells

In the following analyses, we used the tongue muscle to study the mechanism of WNT/β-catenin signaling in *Ctnnb1^{F/F};Myog-Cre* and control mice because it is the most differentiated muscle at birth and also because muscular defects are most apparent in the tongue of *Ctnnb1^{F/F};Myog-Cre* mice compared with controls. There were at least three possibilities to explain these tongue muscle developmental defects: a cell proliferation defect, increased apoptosis and a differentiation defect. To test whether WNT/β-catenin signaling is crucial for cell proliferation, we performed a BrdU incorporation assay, which showed no proliferation defect in *Ctnnb1^{F/F};Myog-Cre;ZsGreen^{cKI/cKI}* mice (Fig. 2A-C; Fig. S2). Next, we conducted terminal deoxynucleotidyl transferase dUTP nick-end labeling (TUNEL) assays to examine apoptosis in *Ctnnb1^{F/F};Myog-Cre;ZsGreen^{cKI/cKI}* and *Ctnnb1^{F/+};Myog-Cre; ZsGreen^{cKI/cKI}* control mice. The number of TUNEL-positive cells in *Ctnnb1^{F/F};Myog-Cre;ZsGreen^{cKI/cKI}* mice was comparable with that of *Ctnnb1^{F/+};Myog-Cre;ZsGreen^{cKI/cKI}* control littermates (Fig. 2D,E). To test whether WNT/β-catenin signaling is crucial for muscle differentiation, we performed quantitative RT-PCR analyses of muscle differentiation markers: the myogenic factor 5 (*Myf5*), myogenic differentiation 1 (*Myod1*, also known as *MyoD*), *Myf6* (also known as *Mrf4*) and *Myog* genes. We found that the expression of *Myf5*, *Myod1*, *Myf6* and *Myog* was significantly downregulated in the tongue of *Ctnnb1^{F/F};Myog-Cre* mice compared with controls at E13.5 and E14.5 (Fig. 2F). In addition, we found that the number of muscle fibers was decreased in *Ctnnb1^{F/F};Myog-Cre;ZsGreen^{cKI/cKI}* mice compared with *Ctnnb1^{F/+};Myog-Cre;ZsGreen^{cKI/cKI}* control mice (Fig. 2G,H); the muscle fibers in *Ctnnb1^{F/F};Myog-Cre;ZsGreen^{cKI/cKI}* mice were thinner (Fig. 2I,J). Moreover, the ratio of mononucleated cells was increased in *Ctnnb1^{F/F};Myog-Cre;ZsGreen^{cKI/cKI}* mice compared with *Ctnnb1^{F/+};Myog-Cre;ZsGreen^{cKI/cKI}* control mice (Fig. 2K). Thus, WNT/β-catenin signaling plays a crucial role in myoblast fusion during muscle development. To test whether our *in vivo* findings were conserved in culture conditions, we performed muscle differentiation assays using primary myoblasts derived from the developing tongue of wild-type control and *Ctnnb1^{F/F};Myog-Cre* mice. Whereas wild-type myoblasts fused and differentiated

into myofibers 5 days after the induction of muscle differentiation, *Ctnnb1^{F/F};Myog-Cre* myoblasts displayed fusion defects during muscle differentiation (Fig. 3A-D; Fig. S3). The fusion index (percentage of nuclei inside the myotubes) showed significant reduction of fused cells in *Ctnnb1^{F/F};Myog-Cre* myoblasts (Fig. 3B). Correlated with the fusion defects, the length of muscle fibers labeled with myosin heavy chain 1 (MYH1) was significantly reduced in *Ctnnb1^{F/F};Myog-Cre* myoblasts compared with control myoblasts (Fig. 3C). Whereas at least 40% MYH1-positive cells were multi-nucleated in wild-type control cells, 90% MYH1-positive cells were mono-nucleated in *Ctnnb1^{F/F};Myog-Cre* myoblasts (Fig. 3D). Taken together, our results indicate that WNT/β-catenin signaling plays a crucial role in myoblast fusion during muscle development.

Identification of the muscle-specific WNT/β-catenin signaling cascade and target molecules

To identify downstream target genes of WNT/β-catenin signaling in muscle fusion, we conducted quantitative RT-PCR analyses of fusion molecules [*Nphs1*, *Ptk2*, *Fermt2*, *Adam12*, *Itga3*, *Itgb1*, *Cdh2*, *Cdh15*, *Myof*, *Dys* (*Dmd*), *Tmem8c* (*Mymk*) and *Gm7325* (*Mymx*)]. Among them, *Nphs1* expression was specifically and significantly downregulated in the tongue of E13.5 *Ctnnb1^{F/F}; Myog-Cre* mice compared with wild-type littermates (Fig. 4A). The gene and protein expression of *Nphs1* was also downregulated in cultured myoblasts isolated from *Ctnnb1^{F/F};Myog-Cre* tongues compared with wild-type controls without inhibition of myogenic differentiation factors (Fig. 4B,C). In wild-type control mice, NPHS1 was expressed in the plasma membrane of tongue muscle cells at E13.5 and E14.5. By contrast, NPHS1 expression was decreased in tongue muscle cells in *Ctnnb1^{F/F};Myog-Cre* mice compared with littermate controls (Fig. S4). To examine whether WNT/β-catenin signaling directly regulated *Nphs1* expression, we conducted a bioinformatics promoter analysis of the *Nphs1* gene. The *Nphs1* promoter region (up to 5 kb upstream of the *Nphs1* gene transcription start site) contained a putative WNT/β-catenin response element (CAAAG, −4082 to −3578) conserved in all eight species examined (mouse, rat, dog, horse, chimpanzee, orangutan and human) (Fig. S5). To validate the binding of β-catenin to the promoter region of the *Nphs1* gene, we conducted a chromatin immunoprecipitation (ChIP) assay for β-catenin binding to the *Nphs1* promoter regions. As expected, β-catenin bound to the WNT/β-catenin response element in wild-type control myoblasts but failed to bind to the response element in *Ctnnb1^{F/F};Myog-Cre* myoblasts (Fig. 4D). Finally, in order to investigate the functional significance of *Nphs1* in myoblast fusion, we carried out rescue experiments in cultured myoblasts. The overexpression of *Nphs1* by the *Nphs1* expression vector partially restored myoblast fusion defects in *Ctnnb1^{F/F};Myog-Cre* myoblasts (Fig. 4E). The fusion index was almost normalized after introduction of *Nphs1* into *Ctnnb1^{F/F};Myog-Cre* myoblasts (Fig. 4F). Correlated with the restored fusion defect, the length of muscle fibers was partially restored with *Nphs1* overexpression in myoblasts from *Ctnnb1^{F/F}; Myog-Cre* mice (Fig. 4G). Although more than 90% MYH1-positive cells were mono-nucleated in *Ctnnb1^{F/F};Myog-Cre* myoblasts, multi-nucleated cells were increased up to 40% after *Nphs1* overexpression in *Ctnnb1^{F/F};Myog-Cre* myoblasts (Fig. 4H). Taken together, our findings suggest that *Nphs1* is a downstream target of WNT/β-catenin signaling in myoblast fusion.

Previous studies suggest that noncanonical WNT signaling pathways are also involved in muscle differentiation. For example, WNT3A, a canonical WNT ligand, inhibits cell proliferation and
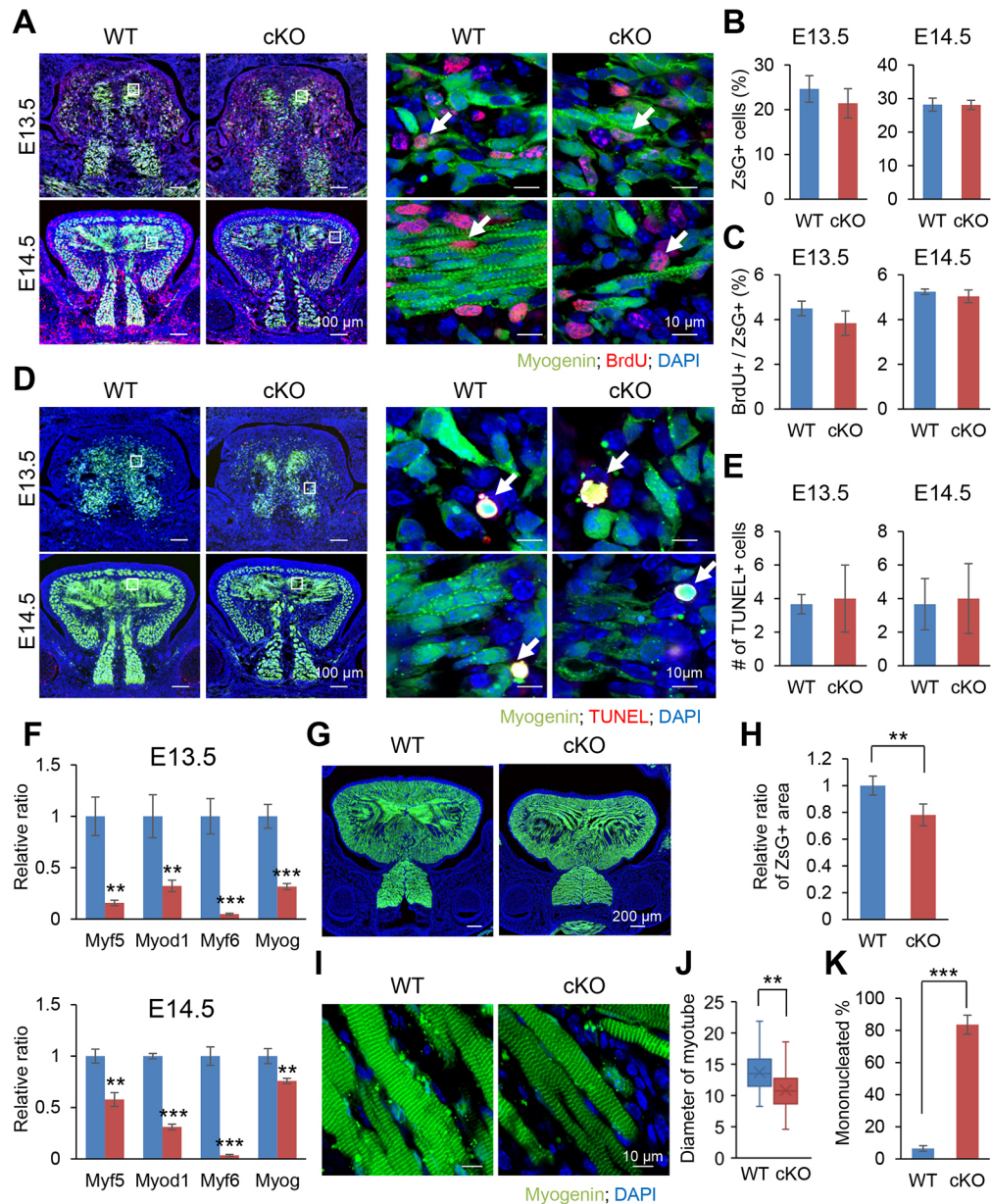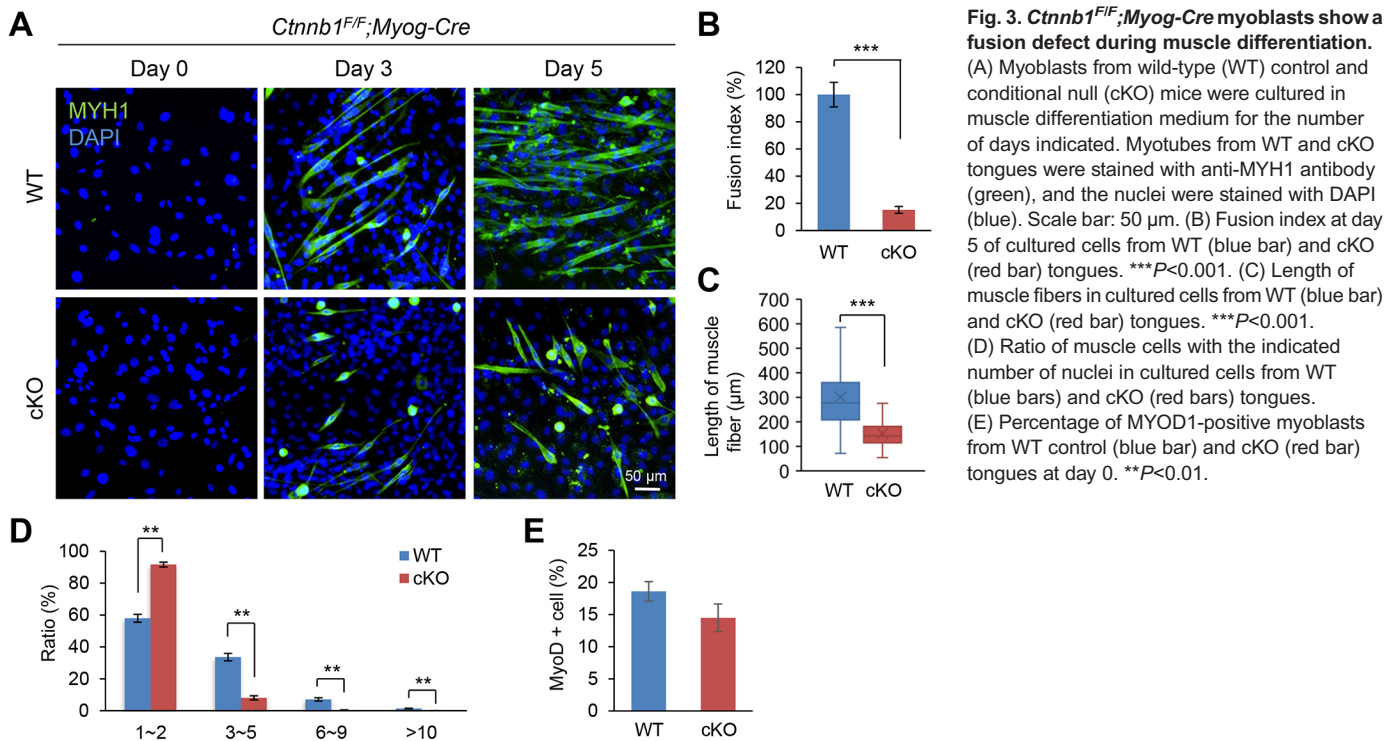
Fig. 2. Loss of β-catenin in the *Myog-Cre*-positive lineage causes a defect in muscle differentiation. (A) BrdU staining of *Myog-Cre;Ctnnb1$^{F/F}$;ZsGreen$^{cKI/cKI}$* (cKO) and *Myog-Cre;Ctnnb1$^{F/+}$;ZsGreen$^{cKI/cKI}$* control (WT) embryos at E13.5 and E14.5. The boxed areas are enlarged in the right panels. Arrows indicate BrdU-positive cells (red). Myog-Cre$^+$ myoblasts are green. Nuclei were counterstained with DAPI (blue). (B) Percentage of ZsGreen-positive cells in the tongue from *Myog-Cre;Ctnnb1$^{F/F}$;ZsGreen$^{cKI/cKI}$* (cKO) and *Myog-Cre;Ctnnb1$^{F/+}$;ZsGreen$^{cKI/cKI}$* control (WT) embryos at E13.5 and E14.5. (C) Percentage of BrdU-positive cells per ZsGreen-positive cells in the tongues from *Myog-Cre;Ctnnb1$^{F/F}$;ZsGreen$^{cKI/cKI}$* (cKO) and *Myog-Cre;Ctnnb1$^{F/+}$;ZsGreen$^{cKI/cKI}$* control (WT) embryos at E13.5 and E14.5. (D) TUNEL staining of *Myog-Cre;Ctnnb1$^{F/F}$;ZsGreen$^{cKI/cKI}$* (cKO) and *Myog-Cre;Ctnnb1$^{F/+}$;ZsGreen$^{cKI/cKI}$* control (WT) embryos at E13.5 and E14.5. The boxed areas are enlarged in the right panels. Arrows indicate TUNEL-positive cells (red). Myogenin-positive myoblasts are green. Nuclei were counterstained with DAPI (blue). (E) Number of TUNEL-positive cells in the tongues from *Myog-Cre;Ctnnb1$^{F/F}$;ZsGreen$^{cKI/cKI}$* (cKO) and *Myog-Cre;Ctnnb1$^{F/+}$;ZsGreen$^{cKI/cKI}$* control (WT) embryos at E13.5 (top) and E14.5 (bottom). (F) Quantitative RT-PCR analyses for muscle differentiation markers in the tongues from *Myog-Cre;Ctnnb1$^{F/F}$;ZsGreen$^{cKI/cKI}$* (cKO) and *Myog-Cre;Ctnnb1$^{F/+}$;ZsGreen$^{cKI/cKI}$* control (WT) embryos at E13.5 and E14.5. **P<0.01; ***P<0.001. (G) Fluorescent images from newborn *Myog-Cre;Ctnnb1$^{F/F}$;ZsGreen$^{cKI/cKI}$* (cKO) and *Myog-Cre;Ctnnb1$^{F/+}$;ZsGreen$^{cKI/cKI}$* control (WT) mice. Myogenin-positive myoblasts are green. Nuclei were counterstained with DAPI (blue). (H) Quantification of the ZsGreen-positive area in the tongue of *Myog-Cre;Ctnnb1$^{F/F}$;ZsGreen$^{cKI/cKI}$* (cKO) and *Myog-Cre;Ctnnb1$^{F/+}$;ZsGreen$^{cKI/cKI}$* control (WT) mice. **P<0.01. (I) Fluorescent images from newborn *Myog-Cre;Ctnnb1$^{F/F}$;ZsGreen$^{cKI/cKI}$* (cKO) and *Myog-Cre;Ctnnb1$^{F/+}$;ZsGreen$^{cKI/cKI}$* control (WT) mice. Myogenin-positive myoblasts are green. Nuclei were counterstained with DAPI (blue). (J) Diameter of ZsGreen-positive myotubes in the tongues of *Myog-Cre;Ctnnb1$^{F/F}$;ZsGreen$^{cKI/cKI}$* (cKO) and *Myog-Cre;Ctnnb1$^{F/+}$;ZsGreen$^{cKI/cKI}$* control (WT) mice. **P<0.01. (K) Percentage of mono-nucleated myotubes in the tongues of *Myog-Cre;Ctnnb1$^{F/F}$;ZsGreen$^{cKI/cKI}$* (cKO) and *Myog-Cre;Ctnnb1$^{F/+}$;ZsGreen$^{cKI/cKI}$* control (WT) mice. ***P<0.001. Scale bars: 100 μm in A,D (left); 10 μm in A,D (right),I; 200 μm in G.

myogenic differentiation in C2C12 cells. On the other hand, WNT7A, a noncanonical WNT ligand, induces cell myogenic differentiation, resulting in hypertrophic myotubes in C2C12 cells and human primary myoblasts derived from satellite cells (von

Maltzahn et al., 2011, 2012b). R-spondin (RSPO), an activator of canonical WNT/β-catenin pathway at the receptor level, regulates a balance/switch between canonical and noncanonical WNT signaling. *Rspo1$^{−/−}$* myoblasts show suppressed canonical

Fig. 3. Ctnnb1$^{F/F}$;Myog-Cre myoblasts show a fusion defect during muscle differentiation.
(A) Myoblasts from wild-type (WT) control and conditional null (cKO) mice were cultured in muscle differentiation medium for the number of days indicated. Myotubes from WT and cKO tongues were stained with anti-MYH1 antibody (green), and the nuclei were stained with DAPI (blue). Scale bar: 50 µm. (B) Fusion index at day 5 of cultured cells from WT (blue bar) and cKO (red bar) tongues. ***$P<0.001$. (C) Length of muscle fibers in cultured cells from WT (blue bar) and cKO (red bar) tongues. ***$P<0.001$. (D) Ratio of muscle cells with the indicated number of nuclei in cultured cells from WT (blue bars) and cKO (red bars) tongues. (E) Percentage of MYOD1-positive myoblasts from WT control (blue bar) and cKO (red bar) tongues at day 0. **$P<0.01$.

WNT/β-catenin signaling and enhanced noncanonical WNT7A-FZD7-RAC1 signaling. The suppression of WNT/β-catenin signaling results in a differentiation defect, and overactivation of non-canonical WNT signaling enhances migration and fusion of myoblasts. During muscle regeneration in adult skeletal muscles, muscles in *Rspo1$^{-/-}$* mice have larger myofibers compared with controls (Lacour et al., 2017). Suppression of *Lgr4*, a RSPO receptor, in C2C12 cells causes defects in myoblast differentiation and fusion due to compromised WNT/β-catenin signaling mediated by RSPO2 (Han et al., 2014). Under hypoxia conditions, canonical WNT/β-catenin signaling is suppressed, but non-canonical WNT7A signaling is activated in C2C12 myoblasts, resulting in hypertrophic myotubes (Cirillo et al., 2017). Treatment with WNT/β-catenin pathway inhibitor XAV939, which promotes phosphorylation and degradation of β-catenin, results in a fusion defect in C2C12 cells (Cirillo et al., 2017), whereas treatment with IWR1-end, a WNT/β-catenin pathway inhibitor, inhibits myoblast fusion in these cells (Suzuki et al., 2015). These studies suggest that the balance between canonical and noncanonical WNT signaling is crucial for proper muscle development *in vitro* and *in vivo*.

The regulation of canonical and noncanonical WNT signaling seems to be more complex at early developmental stages due to crosstalk(s) with other signaling pathways. For example, during early myogenesis at the dermatomyotome, *Myf5* expression is regulated by TCF/β-catenin signaling mediated by Notch, which recruits β-catenin from adherens junctions for translocation into the nuclei during the epithelial-mesenchymal transition (Sieiro et al., 2016). The gain of function of β-catenin also affects myogenesis. For example, mice with constitutive active β-catenin in muscles [*Ctnnb1$^{lox(ex3)/+}$;Myog-Cre* mice] die at birth with a reduced muscle fiber diameter, extra muscle patches on central tendons, and increased nerve defasciculation and branching in the diaphragm (Liu et al., 2012). *Ctnnb1$^{lox(ex3)/+}$;Myf5-Cre* mice exhibit reduced skeletal muscle mass and die at E15.5 (Kuroda et al., 2013). Thus, either too much or too little of WNT/β-catenin

signaling results in impaired myogenesis through crosstalk with other signaling pathways.

Taken together, our data show that WNT signaling regulates myoblast proliferation and differentiation in a spatiotemporal-specific manner. This study provides a better understanding of how WNT/β-catenin signaling regulates the fate of muscle cells during normal muscle development, and of how its disruption can lead to muscle developmental defects. The results from this study may be applied to develop therapeutic approaches that stimulate effective skeletal muscle regeneration following muscle trauma or atrophy.

MATERIALS AND METHODS
Animals

Cell culture
Primary myoblasts were isolated from the tongue and limbs of *Ctnnb1$^{F/F}$; Myog-Cre* mice and control littermates (*n*=6 per group in each experiment). Briefly, for preparing primary myoblast cultures, the tongue and hindlimb muscles were dissected out from newborn mouse embryos and digested in a 2.4 U/ml dispase solution (Gibco) for 1 h at 37°C and 5% CO_2. The digested tissues were then suspended with growth medium [F10 medium supplemented with 20% fetal bovine serum, penicillin, streptomycin and 10 ng/ml bFGF] and the cells were collected by centrifugation. The resuspended cells in growth medium were then placed into a cell culture dish coated with rat collagen type I (MilliporeSigma, C3867) and cultured for up to 7 days at 37°C and 5% CO_2 in a humidified incubator. Myogenic differentiation was induced with muscle differentiation medium [DMEM
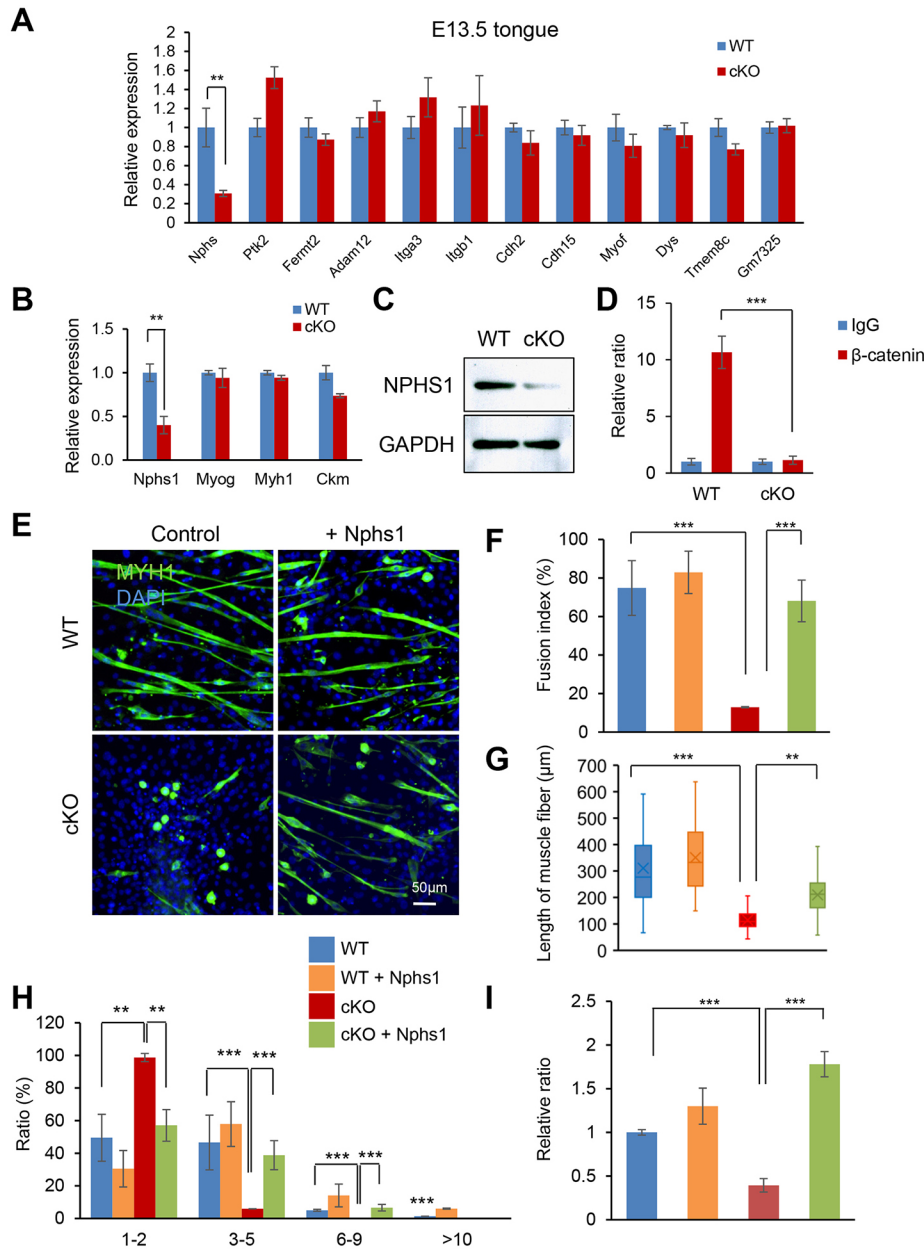
Fig. 4. Nephrin is a downstream target gene of WNT/β-catenin during muscle fusion. (A) Quantitative RT-PCR for the indicated fusion molecules in the tongues from E13.5 wild-type (WT) (blue bars) and conditional null (cKO) (red bars) embryos. **$P<0.01$. (B) Quantitative RT-PCR for *Nphs1*, *Myh1* and *Ckm* in cultured cells from WT (blue bar) and cKO (red bar) tongues. **$P<0.01$. (C) Immunoblotting analysis for NPHS1, with GAPDH as loading control. (D) ChIP assay for β-catenin (red bars) and IgG control (blue bars) in the promoter region of *Nephs1* in cultured cells from WT and cKO tongues. ***$P<0.001$. (E) Muscle differentiation at day 5 after muscle differentiation with *Nphs1* overexpression in cultured cells from WT and cKO mice. Myotubes were stained with MYH1 (green), and nuclei were stained with DAPI (blue). Scale bar: 50 μm. (F) Fusion index at day 5 in cultured cells derived from WT (blue and orange bars) and cKO (red and green bars) tongues with (orange and green bars) or without (blue and red bars) *Nphs1* overexpression. ***$P<0.001$. (G) Length of muscle fibers in cultured cells derived from WT and cKO tongues with or without *Nphs1* overexpression. **$P<0.01$, ***$P<0.001$. (H) Relative ratio of muscle cells with the indicated number of nuclei in cultured cells derived from WT and cKO tongues with or without *Nphs1* overexpression. **$P<0.01$, ***$P<0.001$. (I) Relative ratio of *Nphs1* expression in WT and cKO mice with or without *Nphs1* overexpression. ***$P<0.001$.

supplemented with 2% horse serum, 2 mM L-glutamine, penicillin, streptomycin and insulin (100 ng/ml)] for the period of time indicated. Overexpression of *Nphs1* (Genscript) was determined as previously described (Iwata et al., 2012).

Immunofluorescence analysis

Immunofluorescence analysis was performed as previously described (*n*=3 per group) (Iwata et al., 2013, 2014b; Suzuki et al., 2015), using mouse monoclonal antibodies against MYH1 (MilliporeSigma, M4276, 1:1000) and MYOD1 (Thermo Fisher Scientific, MA5-12902, 1:100), a rabbit polyclonal antibody against NPHS1 (Thermo Fisher Scientific, PA5-20330, 1:100) and a rat monoclonal antibody against active BrdU (Abcam, ab6326, 1:1000); the nuclei were counterstained with DAPI (4′,6′-diamidino-2-phenylinole). The secondary antibodies used were goat anti-mouse Alexa Fluor 488 (Thermo Fisher Scientific, A-11001, 1:500), goat anti-rabbit Alexa Fluor 488 (Thermo Fisher Scientific, A-11008, 1:500), and goat anti-rat Alexa Fluor 568 (Thermo Fisher Scientific, A-11077, 1:500). Fluorescent images were captured by an inverted fluorescent microscope (IX73, Olympus), and confocal images were obtained with a laser confocal scanning microscope (Ti-E, Nikon).

TUNEL assay

Click-iT Plus TUNEL Assay with Alexa 594 (molecular probes, C10618) was used to detect apoptotic cells, according to the manufacturer's instructions, and the confocal images were taken with a laser confocal scanning microscope (Ti-E, Nikon) (*n*=3 per group).

Quantitative RT-PCR

Total RNAs isolated from E13.5 and E14.5 embryonic tongues (*n*=6 per group), and from cultured, differentiated primary myotubes (at day 2) were dissected with the QIAshredder and RNeasy mini extraction kit (QIAGEN), as previously described (Suzuki et al., 2015). The following PCR primers were used for further specific analysis: *Nphs1*, 5′-TGTCATATCGCCAA-GCCTTCA-3′ and 5′-TCTCACACCAGATGTCCCCT-3′; *Ptk2*, 5′-CGC-TGCCTTCTATCTGCCTG-3′ and 5′-TCTTCTGAATGATGCCCCTGAC-3′; *Fermt2*, 5′-GATCACTTTGGAAGGCGGGA-3′ and 5′-GCGCGTAC-TGCTTCTCGTTA-3′; *Adam12*, 5′-AAAGGCTAGACTCGCTGCTC-3′ and 5′-ACGTCTGGATGATCCTTGGC-3′; *Itga3*, 5′-AACAGCACCTTC-ATTGAGGACT-3′ and 5′-GGGGCTGACCCCTCAGTAG-3′; *Itgb1*, 5′-TGCCAAATCTTGCGGAGAATG-3′ and 5′-ACTTCTGTGGTTCTCCTG-ATCT-3′; *Cdh2*, 5′-TTTGTTACCAGCTCGCTCTCAT-3′ and 5′-GCTGA-

ATTTCACATTGAGAAGGGG-3′; *Cdh15*, 5′-AATGAAGGTGTGCTGT-CCGT-3′ and 5′-GTCgTAGTCTTTGGAGTAGCTGA-3′; *Myof*, 5′-CCTC-TGGGGGAGAAGTGGAA-3′ and 5′-GCCTTCGCTGGTACTTCTCAA-3′; *Dys*, 5′-AGCCATAGAATCGAGACTCAGAAC-3′ and 5′-GAGATG CAGAAGCCAGTCCT-3′; *Tmem8c*, 5′-ATCGCTACCAAGAGGCGTT-3′ and 5′-CACAGCACAGACAAACCAGG-3′; *Myf5*, 5′-CGGCATGCCTG AATGTAACAG-3′ and 5′-GCTGGACAAGCAATCCAAGC-3′; *Myod1*, 5′-TGCTCTGATGGCATGATGGATT-3′ and 5′-AGATGCGCTCCACTG-TGCTG-3′; *Myf6*, 5′-GCCAAGGAGGAGAACATGATGA-3′ and 5′-AG-TCTTGCAAGCCCAGATCA-3′; *Myog*, 5′-TCCCAACCCAGGAGATCA-TT-3′ and 5′-AGTTGGGCATGGTTTCGTCT-3′; *Gm7325*, 5′-GTTAGA-ACTGGTGAGCAGGAG-3′ and 5′-CCATCGGGAGCAATGGAA-3′; *Ckm*, 5′-CACCCCTTCATGTGGAACGA-3′ and 5′-CTCAAACTTGGGG-TGCTTGC-3′; and *Gapdh*, 5′-AACTTTGGCATTTGGAAGG-3′ and 5′-ACACATTGGGGGTAGGAACA-3′.

Evaluation of myoblast fusion
After a 5-day culture in differentiation medium, primary myotubes were stained for MYH1 and the nuclei were counterstained with DAPI. The extent of fusion was calculated using the fusion index (Brustis et al., 1994; Honda and Rostami, 1989): fusion %=(number of nuclei in multi-nucleated myotubes)/(total number of nuclei in MYH-positive cells and myotubes)×100, as previously described (Suzuki et al., 2015).

Immunoblotting
Immunoblots were performed as previously described (*n*=3 per group) (Iwata et al., 2010), using a rabbit polyclonal antibody against NPHS1 (Thermo Fisher Scientific, PA5-20330, 1:1000) and a mouse monoclonal antibody against GAPDH (MilliporeSigma, MAB374, 1:5000). A secondary antibody against mouse or rabbit IgG (Cell Signaling Technology, 7976 or 7074) was used at 1:50,000.

Comparative analysis of transcription factor binding site
The UCSC genome browser was used to obtain the genomic sequences of the murine *Nphs1* gene (NC_000073.6), including the 5 kb sequence upstream of the respective transcription start site. The sequence was then mapped to seven additional mammalian genomes [human (Build 38), chimpanzee (Build 2.1.4), orangutan (Build 2.0.2), rhesus macaque (Build 1.0), rat (Build 5), dog (Build 3.1) and horse (Build equCab2)] with the BLAST tool as previously described (Iwata et al., 2013, 2014a). The multiple alignments were obtained using the Clustal Omega tool with default parameters and settings (Sievers et al., 2011). LEF1-binding motifs (minimal core sites: 5′-CTTTG-3′ or 5′-CAAAG-3′; optimal sites: 5′-CTTTGWW-3′ or 5′-WWCAAAG-3′, W=A/T) (Tetsu and McCormick, 1999; van Beest et al., 2000; Yochum et al., 2008) were searched in the aligned DNA sequences.

ChIP assay
E13.5 tongue tissue extracts were incubated with either active β-catenin antibody (Cell Signaling Technology) or IgG overnight at 4°C, followed by precipitation with magnetic beads. Washing and elution of the immune complexes, as well as precipitation of DNA, were performed according to standard procedures, as previously described (*n*=3 per group) (Iwata et al., 2013, 2014a). The putative LEF1 target sites of the *Nphs1* gene in the immune complexes were detected by PCR using the following primers: 5′-TCAAAAGGCTGAGGCAGGAG-3′ (−4082 bp to −4063 bp) and 5′-GCTCATCGCCCCATTTCCTA-3′ (−3576 bp to −3595 bp). The positions of the PCR fragments correspond to NCBI mouse genome Build 38 (mm10).

Statistical analysis
Two-tailed Student's *t*-tests were applied for the statistical analysis. $P \leq 0.05$ was considered statistically significant. For all graphs, data are mean±s.d.

References
Alexander, M. S., Kawahara, G., Motohashi, N., Casar, J. C., Eisenberg, I., Myers, J. A., Gasperini, M. J., Estrella, E. A., Kho, A. T., Mitsuhashi, S. et al. (2013). MicroRNA-199a is induced in dystrophic muscle and affects WNT signaling, cell proliferation, and myogenic differentiation. *Cell Death Differ.* **20**, 1194-1208.

Al-Qattan, M. M. (2011). WNT pathways and upper limb anomalies. *J. Hand Surg. [Am.]* **36**, 9-22.

Borello, U., Berarducci, B., Murphy, P., Bajard, L., Buffa, V., Piccolo, S., Buckingham, M. and Cossu, G. (2006). The Wnt/beta-catenin pathway regulates Gli-mediated Myf5 expression during somitogenesis. *Development* **133**, 3723-3732.

Brault, V., Moore, R., Kutsch, S., Ishibashi, M., Rowitch, D. H., McMahon, A. P., Sommer, L., Boussadia, O. and Kemler, R. (2001). Inactivation of the beta-catenin gene by Wnt1-Cre-mediated deletion results in dramatic brain malformation and failure of craniofacial development. *Development* **128**, 1253-1264.

Braun, T., Rudnicki, M. A., Arnold, H.-H. and Jaenisch, R. (1992). Targeted inactivation of the muscle regulatory gene Myf-5 results in abnormal rib development and perinatal death. *Cell* **71**, 369-382.

Brunelli, S., Relaix, F., Baesso, S., Buckingham, M. and Cossu, G. (2007). Beta catenin-independent activation of MyoD in presomitic mesoderm requires PKC and depends on Pax3 transcriptional activity. *Dev. Biol.* **304**, 604-614.

Brustis, J. J., Elamrani, N., Balcerzak, D., Safwate, A., Soriano, M., Poussard, S., Cottin, P. and Ducastaing, A. (1994). Rat myoblast fusion requires exteriorized m-calpain activity. *Eur. J. Cell Biol.* **64**, 320-327.

Carvajal Mornroy, P. L., Grefte, S., Kuijpers-Jagtman, A. M., Wagener, F. A. and Von den Hoff, J. (2012). Strategies to improve regeneration of the soft palate muscles after cleft palate repair. *Tissue Eng. Part B Rev.* **18**, 468-477.

Chen, J. C. J. and Goldhamer, D. J. (2004). The core enhancer is essential for proper timing of MyoD activation in limb buds and branchial arches. *Dev. Biol.* **265**, 502-512.

Cirillo, F., Resmini, G., Ghiroldi, A., Piccoli, M., Bergante, S., Tettamanti, G. and Anastasia, L. (2017). Activation of the hypoxia-inducible factor 1alpha promotes myogenesis through the noncanonical Wnt pathway, leading to hypertrophic myotubes. *FASEB J.* **31**, 2146-2156.

Cisternas, P., Henriquez, J. P., Brandan, E. and Inestrosa, N. C. (2014a). Wnt signaling in skeletal muscle dynamics: myogenesis, neuromuscular synapse and fibrosis. *Mol. Neurobiol.* **49**, 574-589.

Cisternas, P., Vio, C. P. and Inestrosa, N. C. (2014b). Role of Wnt signaling in tissue fibrosis, lessons from skeletal muscle and kidney. *Curr. Mol. Med.* **14**, 510-522.

Cohen, S. R., Chen, L. L., Burdi, A. R. and Trotman, C. A. (1994). Patterns of abnormal myogenesis in human cleft palates. *Cleft Palate Craniofac. J.* **31**, 345-350.

Cossu, G. and Borello, U. (1999). Wnt signaling and the activation of myogenesis in mammals. *EMBO J.* **18**, 6867-6872.

Dworkin, J. P., Marunick, M. T. and Krouse, J. H. (2004). Velopharyngeal dysfunction: speech characteristics, variable etiologies, evaluation techniques, and differential treatments. *Lang. Speech Hear Serv. Sch.* **35**, 333-352.

Han, X. H., Jin, Y.-R., Tan, L., Kosciuk, T., Lee, J.-S. and Yoon, J. K. (2014). Regulation of the follistatin gene by RSPO-LGR4 signaling via activation of the WNT/beta-catenin pathway in skeletal myogenesis. *Mol. Cell. Biol.* **34**, 752-764.

Hasty, P., Bradley, A., Morris, J. H., Edmondson, D. G., Venuti, J. M., Olson, E. N. and Klein, W. H. (1993). Muscle deficiency and neonatal death in mice with a targeted mutation in the myogenin gene. *Nature* **364**, 501-506.

He, F. and Chen, Y. (2012). Wnt signaling in lip and palate development. *Front. Oral Biol.* **16**, 81-90.

Honda, H. and Rostami, A. (1989). Expression of major histocompatibility complex class I antigens in rat muscle cultures: the possible developmental role in myogenesis. *Proc. Natl. Acad. Sci. USA* **86**, 7007-7011.

DEVELOPMENT

Hutcheson, D. A., Zhao, J., Merrell, A., Haldar, M. and Kardon, G. (2009). Embryonic and fetal limb myogenic cells are derived from developmentally distinct progenitors and have different requirements for beta-catenin. *Genes Dev.* **23**, 997-1013.

Iwata, J.-i., Hosokawa, R., Sanchez-Lara, P. A., Urata, M., Slavkin, H. and Chai, Y. (2010). Transforming growth factor-beta regulates basal transcriptional regulatory machinery to control cell proliferation and differentiation in cranial neural crest-derived osteoprogenitor cells. *J. Biol. Chem.* **285**, 4975-4982.

Iwata, J.-i., Hacia, J. G., Suzuki, A., Sanchez-Lara, P. A., Urata, M. and Chai, Y. (2012). Modulation of noncanonical TGF-beta signaling prevents cleft palate in Tgfbr2 mutant mice. *J. Clin. Invest.* **122**, 873-885.

Iwata, J.-i., Suzuki, A., Pelikan, R. C., Ho, T.-V. and Chai, Y. (2013). Noncanonical transforming growth factor beta (TGFbeta) signaling in cranial neural crest cells causes tongue muscle developmental defects. *J. Biol. Chem.* **288**, 29760-29770.

Iwata, J.-i., Suzuki, A., Pelikan, R. C., Ho, T.-V., Sanchez-Lara, P. A. and Chai, Y. (2014a). Modulation of lipid metabolic defects rescues cleft palate in Tgfbr2 mutant mice. *Hum. Mol. Genet.* **23**, 182-193.

Iwata, J.-i., Suzuki, A., Yokota, T., Ho, T.-V., Pelikan, R., Urata, M., Sanchez-Lara, P. A. and Chai, Y. (2014b). TGFbeta regulates epithelial-mesenchymal interactions through WNT signaling activity to control muscle development in the soft palate. *Development* **141**, 909-917.

Kablar, B., Krastel, K., Ying, C., Asakura, A., Tapscott, S. J. and Rudnicki, M. A. (1997). MyoD and Myf-5 differentially regulate the development of limb versus trunk skeletal muscle. *Development* **124**, 4729-4738.

Kim, N. and Vu, T. H. (2006). Parabronchial smooth muscle cells and alveolar myofibroblasts in lung development. *Birth Defects Res. C Embryo Today* **78**, 80-89.

Kuroda, K., Kuang, S., Taketo, M. M. and Rudnicki, M. A. (2013). Canonical Wnt signaling induces BMP-4 to specify slow myofibrogenesis of fetal myoblasts. *Skelet. Muscle* **3**, 5.

Lacour, F., Vezin, E., Bentzinger, C. F., Sincennes, M.-C., Giordani, L., Ferry, A., Mitchell, R., Patel, K., Rudnicki, M. A., Chaboissier, M.-C. et al. (2017). R-spondin1 controls muscle cell fusion through dual regulation of antagonistic Wnt signaling pathways. *Cell Reports* **18**, 2320-2330.

Li, S., Czubryt, M. P., McAnally, J., Bassel-Duby, R., Richardson, J. A., Wiebel, F. F., Nordheim, A. and Olson, E. N. (2005). Requirement for serum response factor for skeletal muscle growth and maturation revealed by tissue-specific gene deletion in mice. *Proc. Natl. Acad. Sci. USA* **102**, 1082-1087.

Liu, Y., Sugiura, Y., Wu, F., Mi, W., Taketo, M. M., Cannon, S., Carroll, T. and Lin, W. (2012). beta-Catenin stabilization in skeletal muscles, but not in motor neurons, leads to aberrant motor innervation of the muscle during neuromuscular development in mice. *Dev. Biol.* **366**, 255-267.

MacDonald, B. T., Tamai, K. and He, X. (2009). Wnt/beta-catenin signaling: components, mechanisms, and diseases. *Dev. Cell* **17**, 9-26.

Madisen, L., Zwingman, T. A., Sunkin, S. M., Oh, S. W., Zariwala, H. A., Gu, H., Ng, L. L., Palmiter, R. D., Hawrylycz, M. J., Jones, A. R. et al. (2010). A robust and high-throughput Cre reporting and characterization system for the whole mouse brain. *Nat. Neurosci.* **13**, 133-140.

Maretto, S., Cordenonsi, M., Dupont, S., Braghetta, P., Broccoli, V., Hassan, A. B., Volpin, D., Bressan, G. M. and Piccolo, S. (2003). Mapping Wnt/beta-catenin signaling during mouse development and in colorectal tumors. *Proc. Natl. Acad. Sci. USA* **100**, 3299-3304.

Maroto, M., Reshef, R., Munsterberg, A. E., Koester, S., Goulding, M. and Lassar, A. B. (1997). Ectopic Pax-3 activates MyoD and Myf-5 expression in embryonic mesoderm and neural tissue. *Cell* **89**, 139-148.

Munsterberg, A. E., Kitajewski, J., Bumcrot, D. A., McMahon, A. P. and Lassar, A. B. (1995). Combinatorial signaling by Sonic hedgehog and Wnt family members induces myogenic bHLH gene expression in the somite. *Genes Dev.* **9**, 2911-2922.

Noden, D. M. and Francis-West, P. (2006). The differentiation and morphogenesis of craniofacial muscles. *Dev. Dyn.* **235**, 1194-1218.

Perry, J. L. (2011). Anatomy and physiology of the velopharyngeal mechanism. *Semin. Speech Lang.* **32**, 83-92.

Precious, D. S. and Delaire, J. (1993). Clinical observations of cleft lip and palate. *Oral. Surg. Oral. Med. Oral. Pathol.* **75**, 141-151.

Rawls, A., Morris, J. H., Rudnicki, M., Braun, T., Arnold, H.-H., Klein, W. H. and Olson, E. N. (1995). Myogenin's functions do not overlap with those of MyoD or Myf-5 during mouse embryogenesis. *Dev. Biol.* **172**, 37-50.

Rudnicki, M. A., Braun, T., Hinuma, S. and Jaenisch, R. (1992). Inactivation of MyoD in mice leads to up-regulation of the myogenic HLH gene Myf-5 and results in apparently normal muscle development. *Cell* **71**, 383-390.

Rudnicki, M. A., Schnegelsberg, P. N. J., Stead, R. H., Braun, T., Arnold, H.-H. and Jaenisch, R. (1993). MyoD or Myf-5 is required for the formation of skeletal muscle. *Cell* **75**, 1351-1359.

Sieiro, D., Rios, A. C., Hirst, C. E. and Marcelle, C. (2016). Cytoplasmic NOTCH and membrane-derived beta-catenin link cell fate choice to epithelial-mesenchymal transition during myogenesis. *Elife* **5**, e14847.

Sievers, F., Wilm, A., Dineen, D., Gibson, T. J., Karplus, K., Li, W., Lopez, R., McWilliam, H., Remmert, M., Soding, J. et al. (2011). Fast, scalable generation of high-quality protein multiple sequence alignments using Clustal Omega. *Mol. Syst. Biol.* **7**, 539.

Soriano, P. (1999). Generalized lacZ expression with the ROSA26 Cre reporter strain. *Nat. Genet.* **21**, 70-71.

Suzuki, A., Pelikan, R. C. and Iwata, J. (2015). WNT/beta-catenin signaling regulates multiple steps of myogenesis by regulating step-specific targets. *Mol. Cell. Biol.* **35**, 1763-1776.

Tajbakhsh, S., Rocancourt, D., Cossu, G. and Buckingham, M. (1997). Redefining the genetic hierarchies controlling skeletal myogenesis: Pax-3 and Myf-5 act upstream of MyoD. *Cell* **89**, 127-138.

Tetsu, O. and McCormick, F. (1999). Beta-catenin regulates expression of cyclin D1 in colon carcinoma cells. *Nature* **398**, 422-426.

van Beest, M., Dooijes, D., van De Wetering, M., Kjaerulff, S., Bonvin, A., Nielsen, O. and Clevers, H. (2000). Sequence-specific high mobility group box factors recognize 10-12-base pair minor groove motifs. *J. Biol. Chem.* **275**, 27266-27273.

von Maltzahn, J., Bentzinger, C. F. and Rudnicki, M. A. (2011). Wnt7a-Fzd7 signalling directly activates the Akt/mTOR anabolic growth pathway in skeletal muscle. *Nat. Cell Biol.* **14**, 186-191.

von Maltzahn, J., Chang, N. C., Bentzinger, C. F. and Rudnicki, M. A. (2012a). Wnt signaling in myogenesis. *Trends Cell Biol.* **22**, 602-609.

von Maltzahn, J., Renaud, J. M., Parise, G. and Rudnicki, M. A. (2012b). Wnt7a treatment ameliorates muscular dystrophy. *Proc. Natl. Acad. Sci. USA* **109**, 20614-20619.

Yamane, A. (2005). Embryonic and postnatal development of masticatory and tongue muscles. *Cell Tissue Res.* **322**, 183-189.

Yochum, G. S., Cleland, R. and Goodman, R. H. (2008). A genome-wide screen for beta-catenin binding sites identifies a downstream enhancer element that controls c-Myc gene expression. *Mol. Cell. Biol.* **28**, 7368-7379.

Zhong, Z., Zhao, H., Mayo, J. and Chai, Y. (2015). Different requirements for Wnt signaling in tongue myogenic subpopulations. *J. Dent. Res.* **94**, 421-429.